

# The Nuts and Bolts of SARS-CoV-2 Spike Receptor-Binding Domain Heterologous Expression

Mariano Maffei <sup>1,\*</sup>, Linda Celeste Montemiglio <sup>2</sup>, Grazia Vitagliano <sup>3</sup>, Luigi Fedele <sup>3,†</sup>, Shaila Sellathurai <sup>3</sup>, Federica Bucci <sup>3</sup>, Mirco Compagnone <sup>4</sup>, Valerio Chiarini <sup>3</sup>, Cécile Exertier <sup>5</sup>, Alessia Muzi <sup>3</sup>, Giuseppe Roscilli <sup>1,3</sup>, Beatrice Vallone <sup>5</sup> and Emanuele Marra <sup>1,3,\*</sup>

<sup>1</sup> Evvivax Biotech, Via di Castel Romano 100, 00128 Rome, Italy; roscilli@takisbiotech.it

<sup>2</sup> Institute of Molecular Biology and Pathology (IBPM), National Research Council, c/o Department of Biochemical Sciences "Alessandro Rossi Fanelli", Sapienza, University of Rome, P. le Aldo Moro, 5, 00185 Rome, Italy; lindac.montemiglio@uniroma1.it

<sup>3</sup> Takis Biotech, Via di Castel Romano 100, 00128 Rome, Italy; vitagliano@takisbiotech.it (G.V.); luigidxx@gmail.com (L.F.); sellathurai@takisbiotech.it (S.S.); bucci@takisbiotech.it (F.B.); chiarini@takisbiotech.it (V.C.); muzi@takisbiotech.it (A.M.)

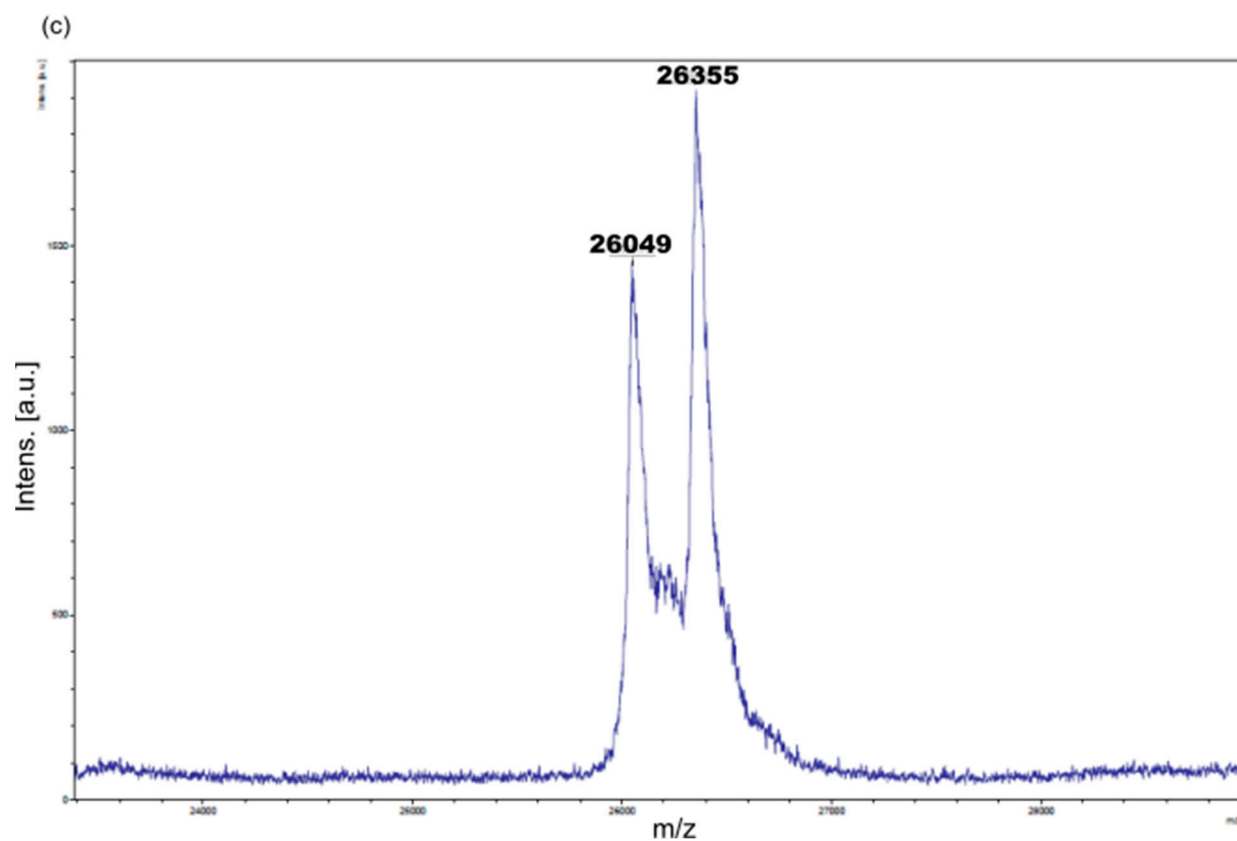
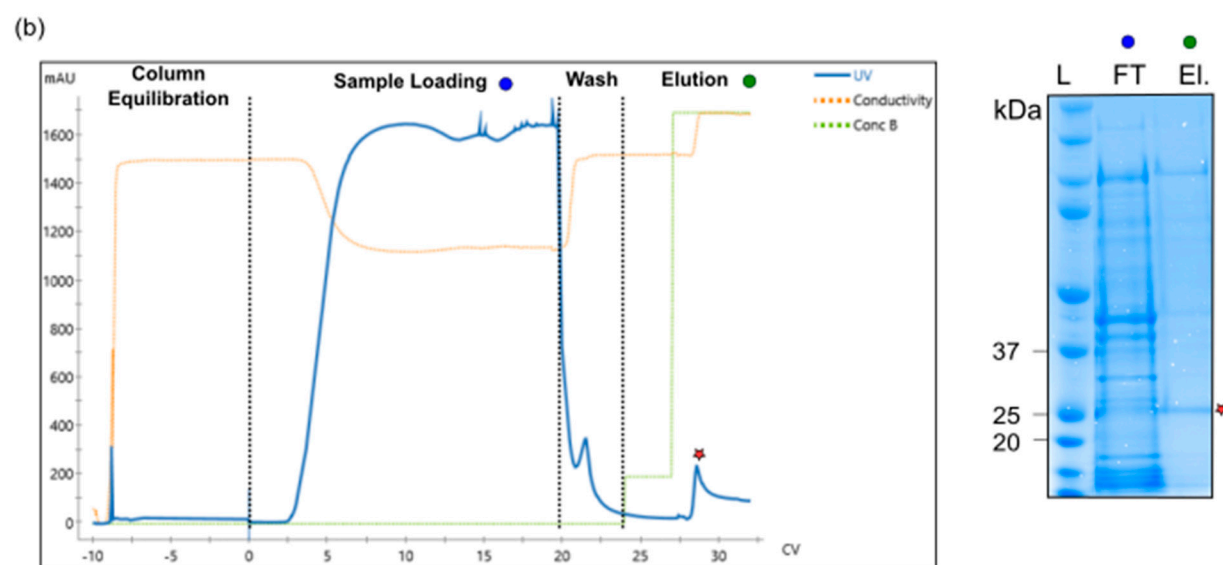
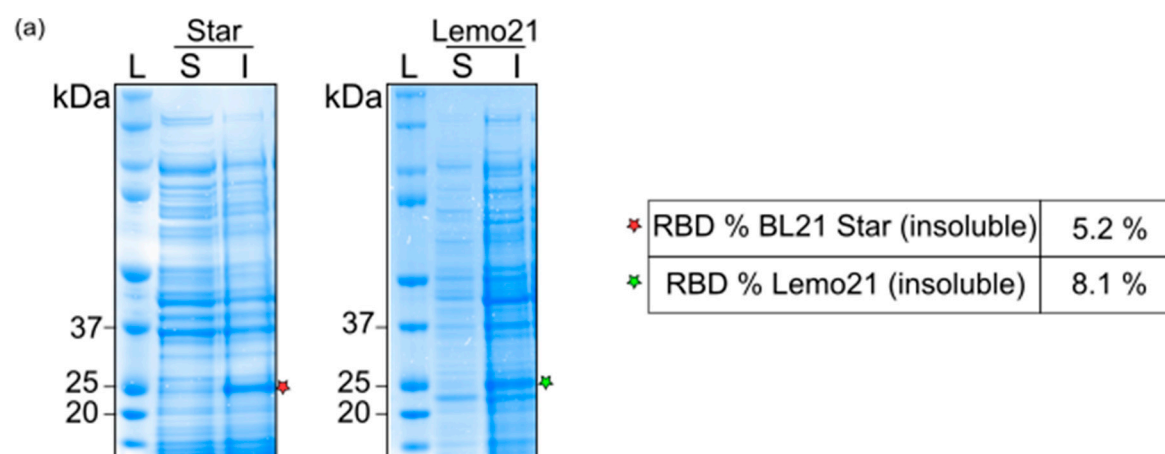
<sup>4</sup> Neomatrix Biotech, Via di Castel Romano 100, 00128 Rome, Italy; compagnone@takisbiotech.it

<sup>5</sup> Department of Biochemical Sciences "Alessandro Rossi Fanelli", Sapienza, University of Rome, P. le Aldo Moro, 5, 00185 Rome, Italy; cecile.exertier@uniroma1.it (C.E.); beatrice.vallone@uniroma1.it (B.V.)

\* Correspondence: maffei@takisbiotech.it (M.M.); marra@takisbiotech.it (E.M.)

† Present address: Luigi Fedele, InnovaVector s.r.l., Via Campi Flegrei 34, 80078, Pozzuoli, Italy.

## SUPPLEMENTARY MATERIAL



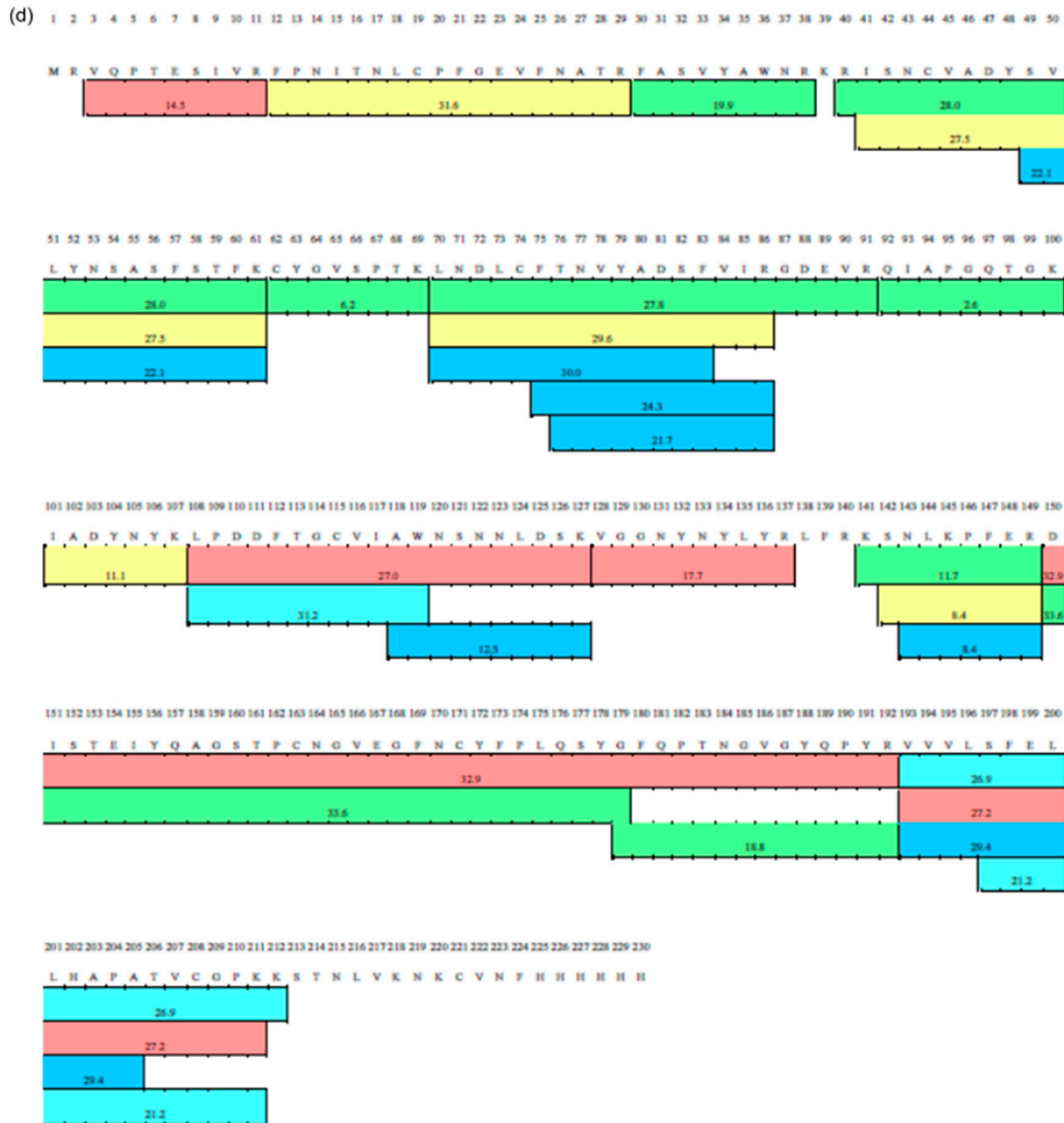
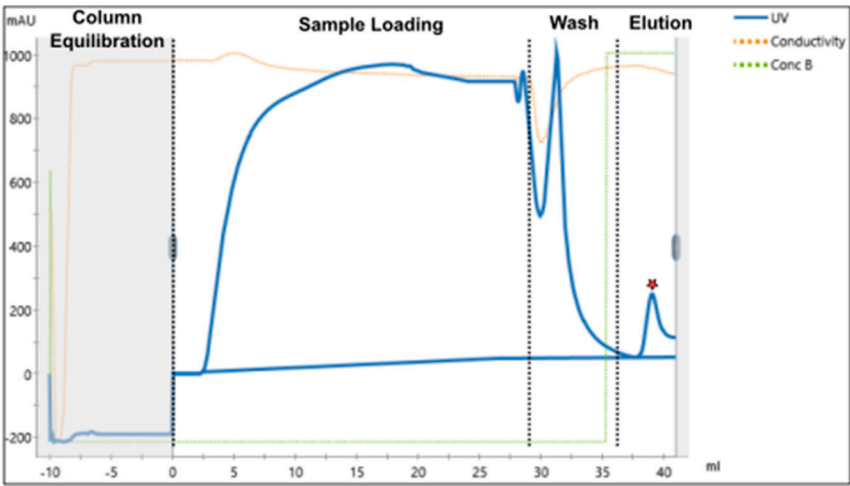
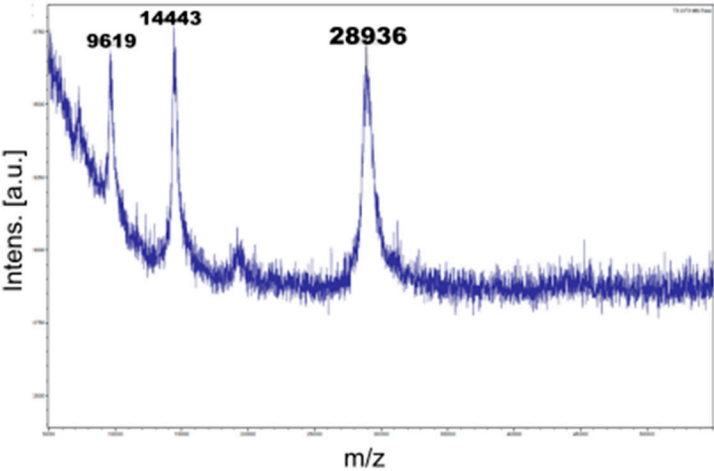


**Figure S1.** *E. coli*-RBD expression and purification. (a) SDS-PAGE analysis of the soluble (S) and insoluble fractions (I) from RBD expression in BL21 Star strain (left) and Lemo21 (right) L= molecular weight ladder. (b) Chromatogram profile of IMAC purification under denaturing conditions of RBD protein (left) and corresponding SDS-PAGE (4-12%) analysis of flow through (FT) and elution (El) fractions. (c) MALDI mass spectrum of RBD sample produced in *E. coli*. (d) Schematic view of recombinant RBD sequence coverage. Protein of interest was represented by its aminoacidic sequence in FASTA and a colored frame in correspondence to each peptide experimentally identified was reported. The rainbow color of the frame is related to the signal intensity, the red one being the most intense and the blue one the lowest. The peptide mass fingerprint (PMF) was determined considering both the molecular weight (from the full mass) and the fragmentation (from the MS/MS mass spectra) of all the peptides detected in the LC-MS/MS analysis of each sample. The result obtained, expressed as sequence coverage (%) for the recombinant *E. coli*-RBD protein, was 89.6%.

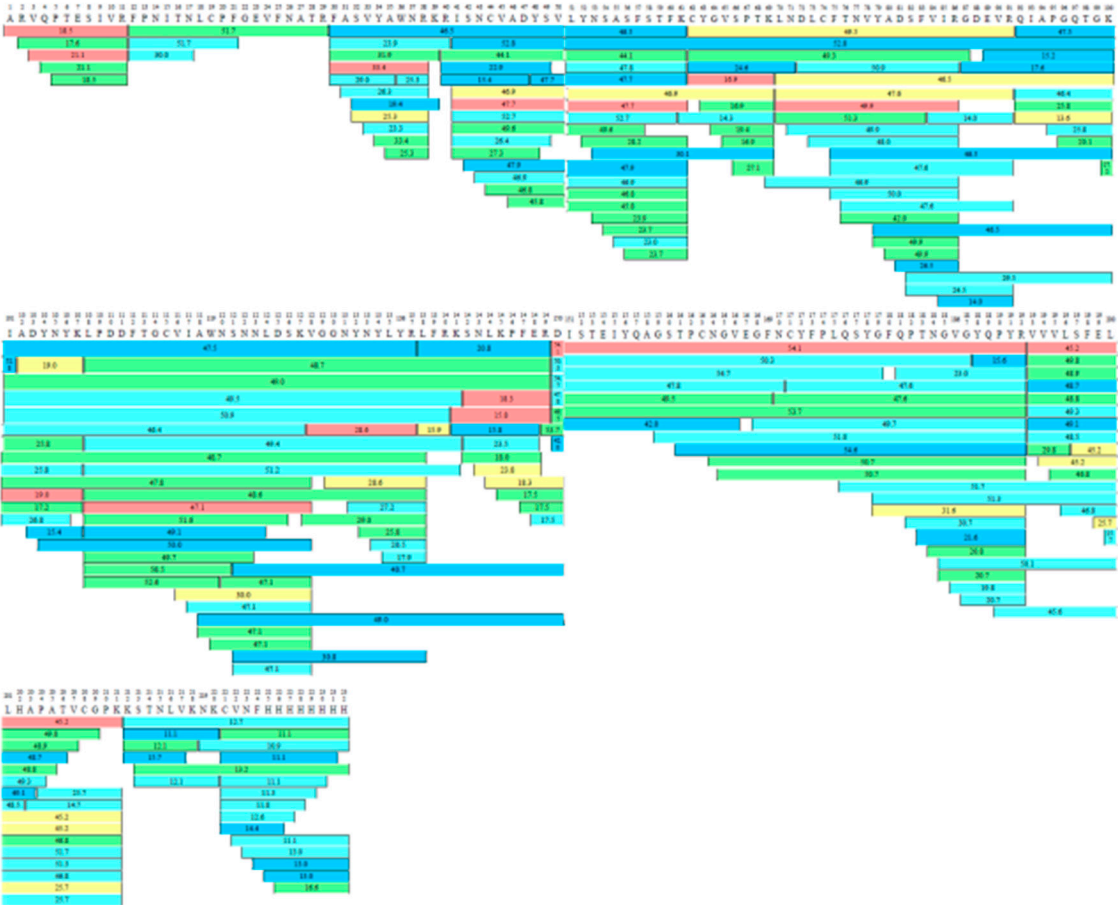
(a)



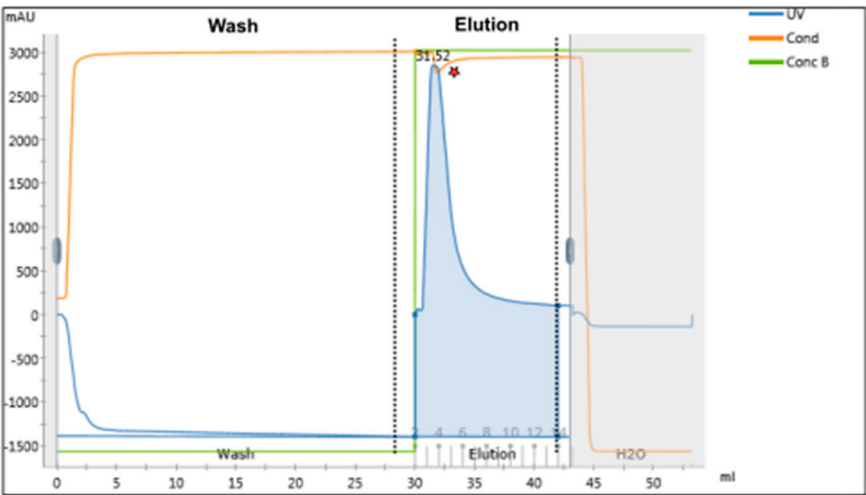
(b)



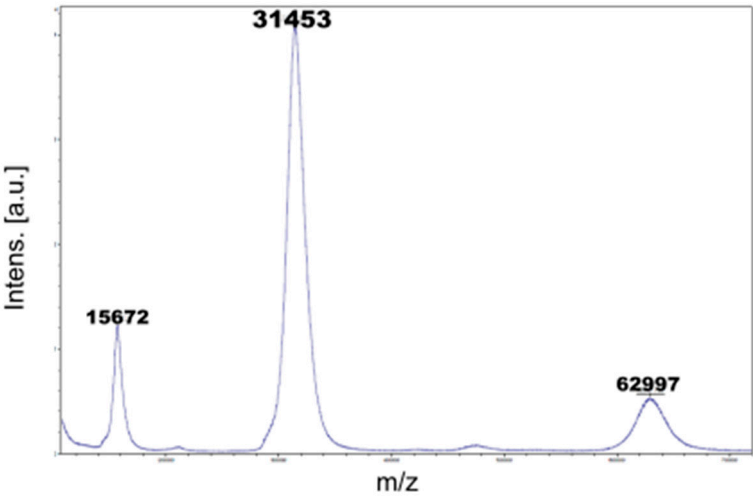
(c)



(d)



(e)



(f)

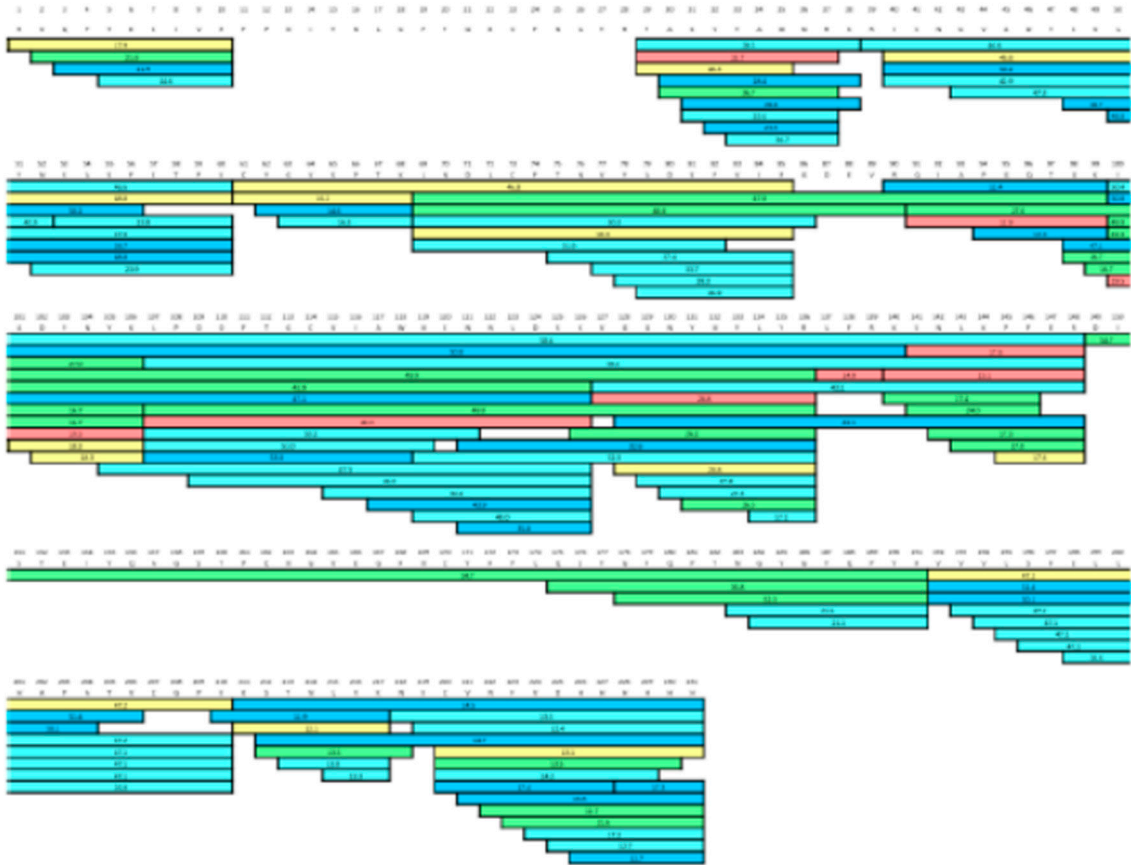


**Figure S2.** Insect-RBD and HEK-293-RBD expression and purification. (a) Chromatogram profile of IMAC purification of RBD protein secreted from Hi-5 cells. (b) MALDI mass spectrum of RBD sample produced in insect cells. The main peak ( $m/z$  28936) corresponds to glycosylated RBD, while the peaks at  $m/z$  14433 and 9619 are attributable to doubly and triply charged species of the same protein. (c) Schematic view of recombinant insect-RBD sequence coverage. The peptide mass fingerprint (PMF) was determined considering both the molecular weight (from the full mass) and the fragmentation (from the MS/MS mass spectra) of all the peptides detected in the LC-MS/MS analysis of each sample. The result obtained, expressed as sequence coverage (%) for the recombinant RBD protein (insect), was 100%. (d) Chromatogram profile of the IMAC purification of RBD protein secreted from mammalian HEK-293. (e) MALDI mass spectrum of RBD sample produced in HEK-293. The mass spectrum showed a main peak at  $m/z$  31453 (glycosylated RBD), a doubly charge species at  $m/z$  15672 and a dimeric species (formed inside the mass spectrometer) at  $m/z$  62997. (f) Schematic view of recombinant HEK-293-RBD sequence coverage. The peptide mass fingerprint (PMF) was determined considering both the molecular weight (from the full mass) and the fragmentation (from the MS/MS mass spectra) of all the peptides detected in the LC-MS/MS analysis of each sample. The result obtained, expressed as sequence coverage (%) for the recombinant RBD protein (insect), was 92.2%. The protein(s) was represented by its aminoacidic sequence in FASTA and a colored frame in correspondence to each peptide experimentally identified was reported. The rainbow color of the frame indicates signal intensity (red is the most intense signal, blue is the lowest one).

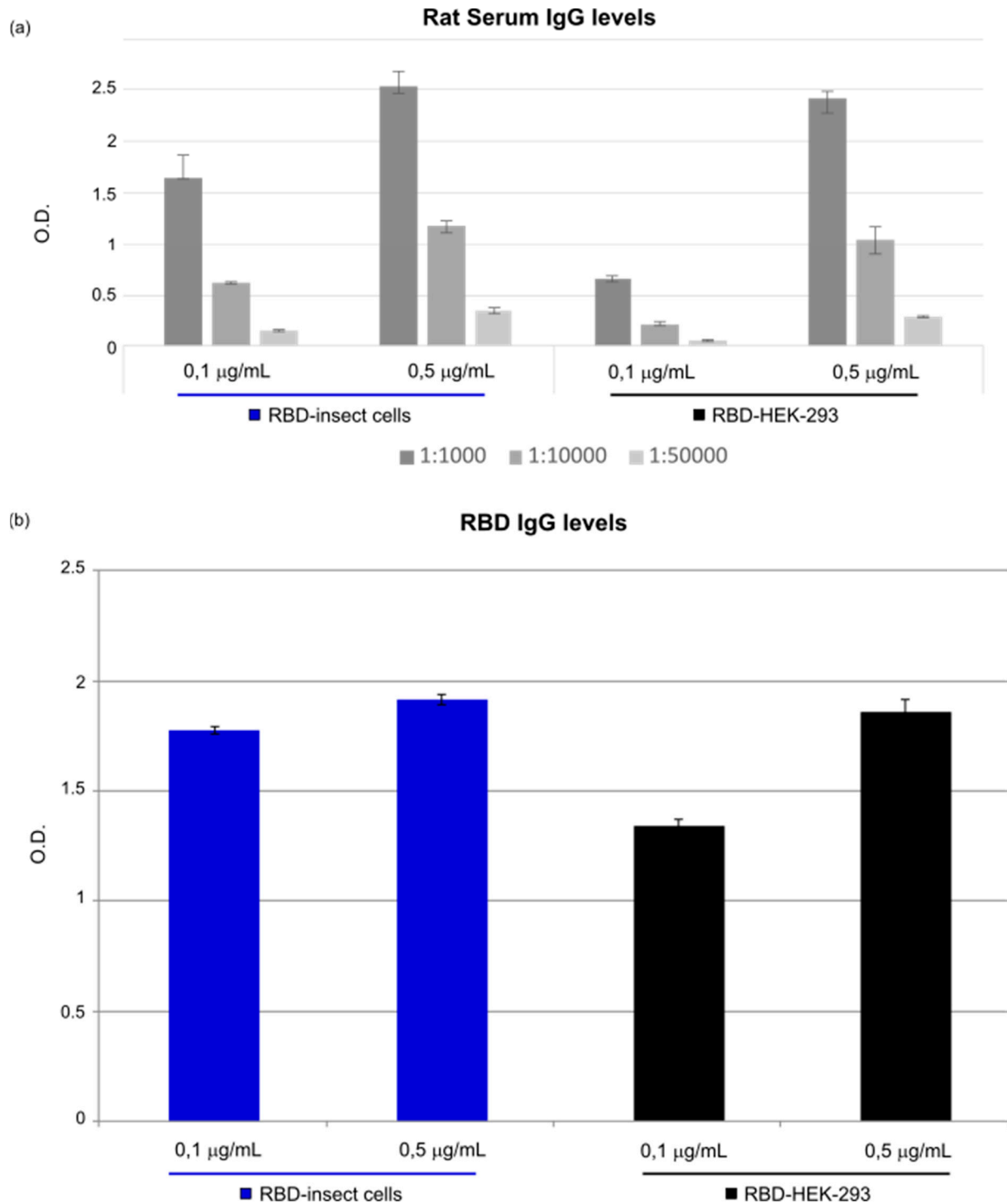
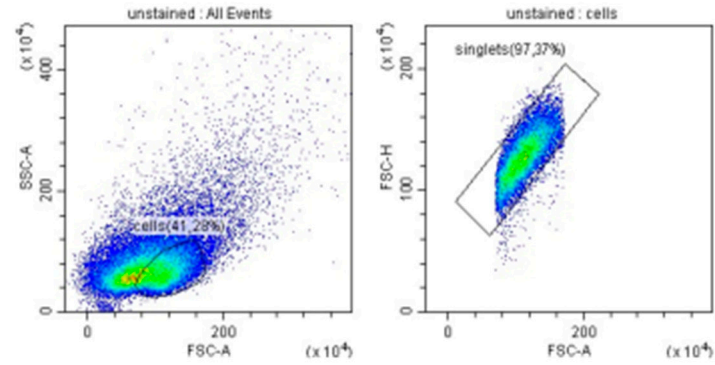
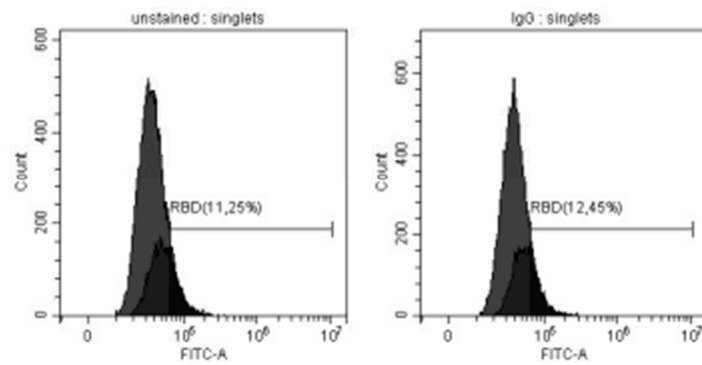


**Figure S3.** ELISA assay (a) Serum from immunized rat against Covid-19 was used to compare different concentrations (0.1 and 0.5 µg/mL) of RBD produced in insect (blue) and HEK-293 cells (black). Optical density (OD) was measured at 405 nm and it is represented in the y-axis. The x-axis shows the dilution factor for serum samples (1:1000, 1:10000, 1:50000). Bars indicate standard deviations. (b) Commercial antibody against the S1 subunit of SARS-CoV-2 Spike was used to compare different concentrations (0.1 and 0.5 µg/mL) of RBD produced in insect (blue) and HEK-293 cells (black). Optical density (OD) was measured at 450 nm and bars indicate standard deviations.

(a)



(b)



(c)

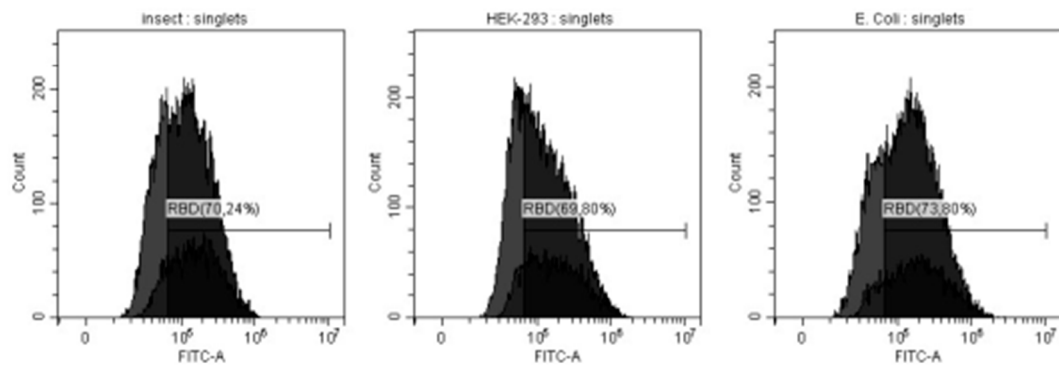


**Figure S4.** FACS data. Representative flow cytometry plots showing (a) gating strategy: dead cells were excluded by their distinctive smaller size (FSC-A) and single cells gated using FSC-H/FSC-A gating. (b) Vero E6 cells alone (left) or incubated only with the secondary antibody (right). (c) Vero E6 cells incubated with insect-RBD (left panel), HEK-293-RBD (middle panel) and E. coli-RBD (right panel) followed by anti-RBD primary antibody and secondary antibody.



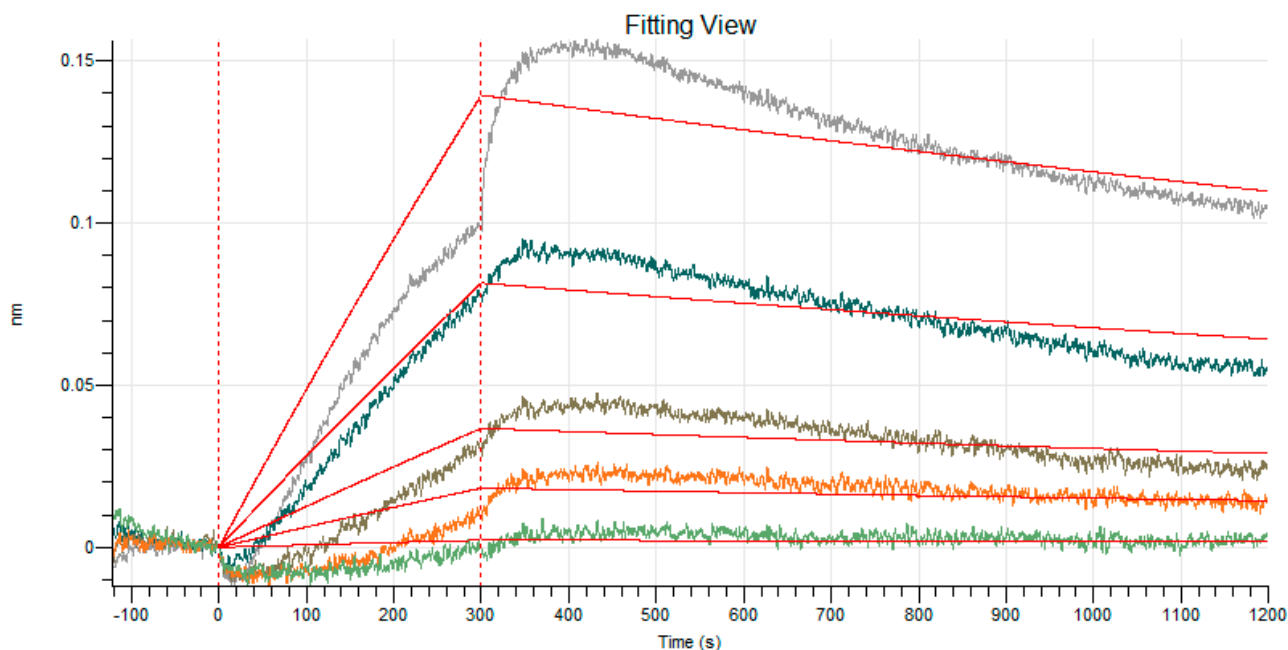


**Figure S5.** BLI data for the binding of E. coli-RBD to ACE2-Fc. After a baseline step, sensorgram starts with the association (0 - 300 s) of RBD on the ACE2 sensor, followed by the dissociation phase (900 s).

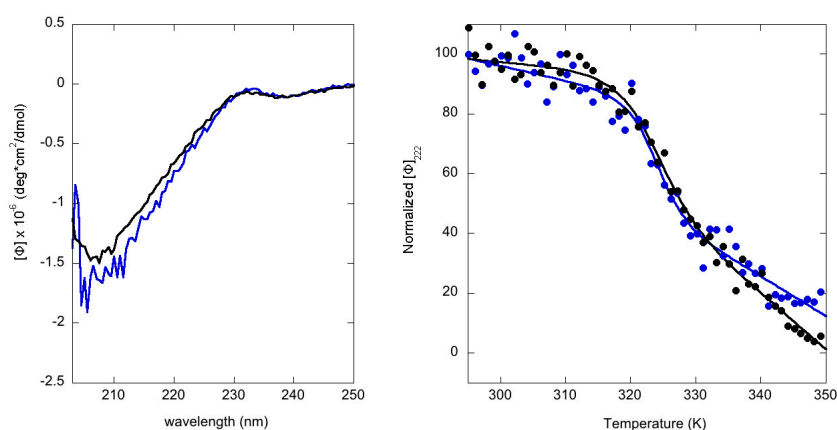


**Figure S6.** CD spectra of HEK-293-RBD. On the left, far-UV CD spectra of HEK-293-RBD obtained in PBS (black) and in 50 mM Tris-HCl, 150 mM NaCl (blue). The spectra were collected at 20°C, using a 0.1 cm path length quartz cuvette. On the right, thermal denaturation profiles of HEK-293-RBD obtained in PBS (black) and in 50 mM Tris-HCl, 150 mM NaCl (blue) continuously monitored by far-UV CD at 222 nm over the range 293–350 K. Data were fitted using a two-state model. A part of a slight increase of noise, the static CD and the thermal unfolding profile obtained in the two buffer conditions are nearly identical, returning similar thermodynamic parameters (HEK-293-RBD in Tris buffer gave:  $T_m = 323.5 \pm 0.8$  K;  $\Delta H_{T_m} = 90 \pm 27$  kcal mol<sup>-1</sup>;  $\Delta G_{n-u}$  @ 295 K  $\sim 4.0$  kcal mol<sup>-1</sup>).

RBD (aa 319-541) expression organism	Buffer conditions	T <sub>m</sub> (K)	ΔH <sub>Tm</sub> (kcal mol <sup>-1</sup> )	ΔG <sub>D-N</sub> (kcal mol <sup>-1</sup> ) @ 295 K
HEK-293	PBS	323.3 ± 1.0	67.7 ± 15.6	~ 2.1
Insect	50 mM Tris · HCl 150 mM NaCl	323.8 ± 0.4	75.9 ± 20.6	~ 2.8
<i>E. coli</i>	50 mM Tris · HCl 150 mM NaCl 1 mM TCEP 20% glycerol	319.8 ± 0.2	41.0 ± 11.7	~0.2

**Table S1.** Thermodynamic parameters for the thermal unfolding of SARS-CoV-2 RBD from different expression organisms using far-UV CD. To a first approximation, the thermodynamic parameters of unfolding have been estimated using the  $\Delta C_p$  value reported for  $\alpha$ -chymotrypsin (241 amino acids) [28]. Data are presented as means ± standard deviation of three independent experiments.